Cadmium inhibits cell cycle progression and specifically accumulates in the maize leaf meristem

Cadmium inhibits cell cycle progression and specifically accumulates in the maize (*Zea mays* L.) leaf meristem

Running title (max 60 chars, incl. spaces):

Cd deposition and cell cycle inhibition in the maize leaf

Authors, listed in following order:

1. Jonas Bertels[1] - jonas.bertels@uantwerpen.be
2. Michiel Huybrechts[2] - michiel.huybrechts@uhasselt.be
3. Sophie Hendrix[2] - sophie.hendrix@uhasselt.be
4. Lieven Bervoets[3] - lieven.bervoets@uantwerpen.be
5. Ann Cuypers[2] - ann.cuypers@uhasselt.be
6. Gerrit T.S. Beemster[1*] - gerrit.beemster@uantwerpen.be

[1] Laboratory for Integrated Molecular Plant Physiology Research (IMPRES), University of Antwerp, Groenenborgerlaan 171, 2020 Antwerpen, Belgium

[2] Centre for Environmental Sciences (CMK), Hasselt University, Agoralaan Building D, 3590 Diepenbeek, Belgium

[3] Systemic Physiological and Ecotoxicological Research (SPHERE), University of Antwerp, Groenenborgerlaan 171, 2020 Antwerpen, Belgium

* Corresponding author – telephone number: Gerrit Beemster, **+32 3 265 34 21**

Submission date: 2020/04/04

Total number of figures: 5 (no colour in print required)

Total number of tables: 2

Supplementary data: 2 tables, 6 figures (colour online required for S1, S4 and S5)

Current word count: 6437 (5005 excl. Material and Methods section)

Highlight

Cadmium, taken up from the soil, results in Cd deposition in the maize leaf growth zone and leads to an inhibition of cell cycle progression and cell expansion.

Abstract

It is well known that cadmium (Cd) pollution inhibits plant growth, but how this metal impacts leaf growth processes at the cellular and molecular level is still largely unknown. In the current study, we show that Cd specifically accumulates in the meristematic tissue of the growing maize leaf, while Cd concentration in the elongation zone rapidly declines as the deposition rates diminish and cell volumes increase due to cell expansion. A kinematic analysis shows that, at the cellular level, a lower number of meristematic cells together with a significantly longer cell cycle duration explain the inhibition of leaf growth by Cd. Flow cytometry analysis suggests an inhibition of the G1/S transition, resulting in a lower proportion of cells in the S-phase and reduced endoreduplication in expanding cells under Cd stress. Lower cell cycle activity is also reflected by lower expression levels of key cell cycle genes (*putative wee1*, *cyclin-B2-4* and *minichromosome maintenance4*). Cell elongation rates are also inhibited by Cd, which is possibly linked to the inhibited endoreduplication. Taken together, our results complement studies on Cd-induced growth inhibition in roots and link inhibited cell cycle progression to Cd deposition in the leaf meristem.

Keywords

1. Cadmium
2. Cell cycle
3. Cell division
4. Cell elongation
5. Endoreduplication
6. Gene expression
7. Growth zone
8. Heavy metal
9. Kinematic analysis
10. Meristem

Abbreviations

Cd	Cadmium
MCM4	minichromosome maintenance4 (gene product symbol)
mcm4	*minichromosome maintenance4* (gene locus symbol)
WEE1	putative WEE1 (gene product symbol)
wee1	*putative wee1* (gene locus symbol)
LER	leaf elongation rate

Introduction

At the cellular level, plant growth is driven by cell proliferation and cell expansion. Cell proliferation, rather than cell expansion, determines the final size of organs, as shown by the meta-analysis performed by Gázquez and Beemster (2017). Abiotic stress often causes plants to grow at a slower rate by inhibiting cell division and expansion to varying degrees. For instance, under severe drought stress, maize leaf elongation rate was reduced by 63%, which could partially be explained by an increased cell cycle duration of 84% (Avramova *et al.*, 2015*a*). Also, Kavanová *et al.* (2006) showed that phosphorus deficiency reduced leaf elongation rate by 39% due to decreases in the cell production rate and final cell length. In Arabidopsis, West *et. al.* (2004) showed that salt stress resulted in reduced growth of roots due to a decrease in cell production and mature cell size.

After cells have stopped proliferating, they grow in size, further increasing organ size. In roots, monocotyledonous leaves and hypocotyls, this elongation mainly occurs along the longitudinal axis due to the transverse orientation of the cellulose microfibrils (Green, 1962; Crowell *et al.*, 2011). The increase in cell size is typically accompanied by endoreduplication (Sugimoto-Shirasu and Roberts, 2003). During endoreduplication, cells alternate between G1 and S-phases, skipping mitosis, doubling their genome with each completed S-phase (Sugimoto-Shirasu and Roberts, 2003). Endopolyploidy in plants can also be affected by abiotic stress, where plants typically increase endopolyploidy levels as an adaptive, plastic response to mitigate the effects of stress, as reviewed by Scholes and Paige (2015).

We use the maize leaf model system to study the impact of abiotic stress on organ growth because it allows to combine analyses at cellular, molecular and biochemical levels at high spatial resolution (Avramova *et al.*, 2015*b*). Maize leaf growth is driven by linearly organized growth processes: cell division in the meristem (i.e. a pool of continuously dividing cells, occurring at the base of the leaf typically in the first 1 to 2 centimetres) and cell elongation in the elongation zone (occurring directly apical of the meristem and typically extending over 4 to 6 centimetres) (Avramova *et al.*, 2015*a*). When cells have reached their mature cell length, they enter the mature zone and form the emerged part of the blade. The longitudinal separation of these developmental stages allows sampling of dividing and elongating cells from a single leaf (Nelissen *et al.*, 2013). Moreover, the size of the maize leaf yields sufficient

amounts of tissue for each of these developmental stages for biochemical and molecular analyses, making it an ideal plant system for these analyses (Avramova *et al.*, 2015*b*).

Industrial activities and the use of phosphate fertilizers have caused cadmium (Cd) disposition and accumulation on large surfaces across the world (Nagajyoti *et al.*, 2010). Though Cd is nonessential, plants take up this metal through transporters for essential bivalent cations such as calcium, iron and zinc (Verbruggen *et al.*, 2009). Being a non-redox active metal, Cd may cause oxidative stress indirectly by perturbing the plants' reactive oxygen species (ROS) metabolism (e.g. by inhibiting enzymes which function in antioxidative defence mechanisms (Cuypers *et al.*, 2010)). Despite the extensive antioxidant defence system of plants (Cuypers *et al.*, 2012), Cd stress may inhibit growth by causing ROS induced DNA damage (Hendrix *et al.*, 2018; Huybrechts *et al.*, 2019), impaired cell wall metabolism (Loix *et al.*, 2017), mitotic aberrations (Fusconi *et al.*, 2007; Silva *et al.*, 2013) and inhibited photosynthesis and respiration (Bi *et al.*, 2009).

The impact of Cd on growth and more specifically the cell cycle is mostly studied in synchronised cell cultures and roots that are directly exposed to Cd treatments, as recently reviewed by *Huybrechts et al.* (2019). These studies mainly report a halted cell cycle at G1/S and G2/M transitions. However, studies on how Cd impacts the growth of plant organs that are not directly exposed, especially leaves, are limited.

Therefore, the aim of our research is to determine the mechanism(s) by which Cd inhibits leaf growth, using the maize leaf as a model system. Our 2 key research questions are: 1. Does Cd reach the leaf growth zone and hence directly affect dividing and elongating cells in the growing maize leaf and 2. What is the cellular basis of Cd inhibited leaf growth in maize (i.e. inhibition of cell division and/or cell elongation)? To tackle these research questions, we used a holistic approach, integrating data at the biochemical (i.e. mineral analysis), cellular (i.e. kinematic analysis and flow cytometry) and molecular level (i.e. gene expression analysis). Through this approach we show that Cd accumulates in the division zone of the leaf, where it inhibits cell cycle progression. Cd deposition continues in the elongation zone, where cell elongation rates are reduced, possibly due to an inhibition of the endocycle.

Material and Methods

Seeds, soil preparation and growth conditions

We grew maize plants (*Zea mays* L.*,* B73 inbred line, obtained from the North Central Regional Plant Introduction Station) in a growth chamber under controlled conditions (16-h day/8-h night, 25°C/18°C day/night, 200 $\mu mol \cdot m^{-2} \cdot s^{-1}$ photosynthetically active radiation, provided by high-pressure sodium lamps).

Peat potting medium (57% soil water content, Jiffy Products International B.V., The Netherlands) was spiked with 10 ml distilled water (control treatment) or 10 ml $CdSO_4$ solutions ($3CdSO_4 \cdot 8H_2O$, prepared in distilled water, Table 1). A fixed mass (650 grams) of potting medium was used for each individual pot (2.0L) to which the solutions were added dropwise under continuous mixing with a kitchen mixer (Kenwood kMix KMX50). Immediately after soil preparation, seeds were planted and the pots were placed in the growth room, covered with plastic wrap until germination. Pots were watered daily with tap water to maintain the original soil water content.

Dose-Response and treatment selection

We determined leaf elongation rate and final leaf length of the fifth leaf of plants exposed to 6 Cd concentrations and a control treatment. To this end, leaf length was measured daily with a ruler from its emergence from the whorl of older leaves until it reached maturity and stopped growing. Leaf elongation rate was determined using the first 4 leaf length measurements of each plant, when growth was approximately steady-state.

Based on the dose-response, 3 treatments were selected for use in the subsequent experiments: a control, a mild (46.5 mg Cd · kg^{-1} dry soil) and a severe treatment (372.1 mg Cd · kg^{-1} dry soil). At 24 days after sowing, plants subjected to these treatments show a clear difference in size (Supplementary Fig. S1).

Cadmium mineral analysis

We determined Cd concentrations in one-centimetre segments sampled along the maize leaf growth zone (i.e. 10 centimetres in total) and included a blade segment (middle of the remaining blade). Fresh weight of the sampled leaf segments was measured (AX124,

Sartorius, Göttingen, Germany), after which they were oven-dried at 60 °C for 48 to 72 hours. Hereafter, segments from the same position and treatment were pooled (2-3 segments per pool). Sample digestion was performed by an overnight predigestion in aqua regia (1:3 nitric acid and hydrochloric acid), followed by 20 minutes high pressure high temperature digestion (Discover SP-D, CEM, Matthews, NC, USA), allowing the samples to boil at 200 °C. The samples were then diluted 40 times with trace metal grade ultrapure water, after which the Cd concentration was measured with high resolution inductively coupled plasma mass spectrometry (Element XR, Thermo Scientific, Bremen, Germany). We used blanks to correct for background trace metals and Rye grass European Reference Material CD281 samples as a reference.

Kinematic analysis

We performed a kinematic analysis on the fifth leaf as described by Sprangers *et al.* (2016). After the emergence of the fifth leaf from the whorl of older leaves, its length was measured daily with a ruler. Leaf elongation rate was determined using the first 3 leaf length measurements of each plant. Three days after emergence, 6 plants of each treatment (i.e. control, mild and severe, as determined in the dose-response experiment) were dissected for cell length and meristem size measurements, while the remaining plants (n = 4 to 5) were used to further measure growth until the final leaf length was reached. Cell length measurements (epidermal pavement cells directly adjacent to stomatal files) along the longitudinal axis of the leaf were performed on 1 centimetre sections that were fixed overnight in 70% ethanol and cleared, stored and mounted on slides in lactic acid. Cells were visualized using differential interference contrast microscopy (Zeiss Axio Scope.A1 microscope, Oberkochen, Germany) at 40x magnification and the length of abaxial epidermal cells adjacent to stomatal cell rows was determined using the online measurement module in the Axiovision software (Rel. 4.8, Zeiss). Leaf meristem size was determined using fluorescence microscopy of DAPI-stained (1 µg/ml 4',6-diamidino-2-phenylindole (DAPI) staining solution) leaf sections at 20x magnification by locating the most distal mitotic figure in epidermal pavement cells.

Cadmium flux and deposition

To determine the uptake of Cd along the growth zone we calculated Cd deposition rates using a kinematic approach combining velocity profiles with Cd concentrations in function of position along the growth zone (Meiri *et al.*, 1992). First, we determined cell flux, which is the number of cells passing by at a certain location per unit time. Cell flux outside the meristem was obtained by dividing leaf elongation rate by mature cell length. Inside the meristem, cell flux was set to zero at the base of the meristem, with a linear increase towards the end of the meristem, where cell flux equals the constant cell flux outside the meristem. Then, the velocity profile was obtained by multiplying local flux rates with local cell lengths and smoothed and interpolated using the locpoly function of the KernSmooth package according to Rymen *et al.* (2010). This fit also yields the derivative of the velocity profile that corresponds to local relative cell expansion rates. Finally, the velocity in the middle of each segment was multiplied by the Cd concentration of the same segment and corrected for segment length and number of plants in the pooled sample, yielding the Cd flux. To retain the variance in the velocity and Cd values from separate experiments, velocities from every replicate were multiplied with all corresponding Cd concentrations, yielding a minimum of 24 (6x4) combinations per treatment. Hereafter, the local rate of Cd deposition was obtained as the derivative of this Cd flux using the locpoly function of the KernSmooth package.

Flow cytometry

For each treatment (Table 1), we sampled 10 one-centimetre segments along the maize leaf growth zone (n = 6). Samples were processed as described before (Hendrix *et al.*, 2018) using the CyStain PI Absolute P kit (Sysmex Partec). Using a CyFlow Cube 8 flow cytometer (Sysmex Partec), PI fluorescence intensity was determined using 488 nm excitation and 580 nm detection for a minimum of 7500 nuclei per sample. The number of 2C, 4C nuclei and S-phase nuclei were determined in R (v 3.6.1) using the flowCore package (v 1.50.0, Hahne *et al.* (2009) as described in supplementary Fig. S2).

Quantitative real-time PCR

We measured expression levels of 3 cell cycle genes: *putative wee1-like protein kinase (further referred to as wee1)*, which controls S-phase progression in plants by phosphorylation

of CDKs and arrests S-phase progression under DNA stress (Cools *et al.*, 2011; Hu *et al.*, 2016); *mcm4*, part of the prereplication complex that mediates unwinding the DNA during S-phase (Masai *et al.*, 2010) and *cyclin-B2-4*, a member of the family of positive CDK regulators controlling G2-to-M transition (Scofield *et al.*, 2014). Samples were obtained from the first 5 centimetres of the fifth leaf's growth zone, 3 days after emergence. These 5 centimetres were dissected in 6 half centimetre segments, followed by 2 one-centimetre segments in 3 biological replicates per treatment, each consisting of a pool of 4 plants. Sections were frozen in liquid nitrogen and stored at -80°C. We ground the leaf material with a ball mill grinder (Retsch MM400, Verder NV, Aartselaar, Belgium), using ceramic balls. Total RNA was extracted using the RNeasy Plant mini kit (Qiagen, Hilden, Germany) and diluted to 0.4 $\mu g \cdot \mu L^{-1}$. First strand cDNA synthesis was performed using SuperScript™ II Reverse Transcriptase according to the manufacturer's protocol (Thermo Fisher Scientific, Waltham, Massachusetts, USA). The synthesised cDNA was used for quantitative real-time PCR using the SYBR™ Green Master Mix (Kaneka Eurogentec S.A., Seraing, Belgium). Expression values were normalised using *Zm00001d036201* (hypothetical protein) as reference gene (Supplementary Table S1 for housekeeping gene selection (Lin *et al.*, 2014)). Gene expressions values were calculated using the $2^{-\Delta\Delta C_T}$ method (Livak and Schmittgen, 2001), relative to the expression of the gene in the first segment of the control plants. Primers (Supplementary Table S2) were created using the NCBI primer designing tool available at https://www.ncbi.nlm.nih.gov/tools/primer-blast/ .

Statistics

Statistical analysis was performed in R (v. 3.6.1). For the kinematic analysis, we used a one-way ANOVA or a Kruskal-Wallis test depending whether assumptions for normal distribution (Shapiro-Wilk test) and homoscedasticity (Levene's test) were met. When there was a significant effect of treatment, we performed a Tukey's HSD test or pairwise Wilcoxon rank sum test. For the remaining analyses, a two-way ANOVA was performed (with segment in the growth zone and treatment as factors). When required, data was $\log_{10}$ transformed to improve the distribution or homoscedasticity. For cadmium concentration, flux and deposition statistics, only data for mild and severe treatments were used because cadmium concentrations in the control treatment were close to zero, resulting in a non-normal distribution of the residuals.

Results

Dose-Response

To determine the effect of Cd concentrations in the soil on the growth of maize leaves, we first performed a dose-response growth analysis. For studying the effect of abiotic stress on growth, we routinely study the 5th leaf of maize seedlings because its growth is independent on seed reserves, approximately steady state for about 5 days after emergence and affected by environmental conditions (Avramova *et al.*, 2017).

Leaf elongation rate (LER) was reduced by 25 to 57%, following a progressive, but non-linear decrease with increasing Cd concentrations (Fig. 1A). For all treatments the reduction in final leaf length was approximately half of that of the effect on LER (Fig. 1B), so that the highest dose only reduced final leaf length by 30%. The difference between the LER and final leaf length can be explained by a progressive increase of the duration of leaf elongation with increasing Cd levels, which partially compensates for the lower leaf elongation rate. Based on leaf elongation rate and final leaf length, we selected a mild (i.e. 46.5 mg Cd · kg dry soil^{-1}; inhibiting LER by 25%) and severe treatment (372.1 mg Cd · kg dry soil^{-1}; inhibiting LER by 52%) for further detailed analyses (Table 1).

Cadmium accumulation

Next, we set out to determine whether the growth inhibition could be due to Cd accumulation in the leaf growth zone. Severe Cd stress significantly increased the dry to fresh weight ratio of the leaf material (Supplementary Fig. S3). On a fresh weight basis, Cd levels increased with increasing concentrations in the soil (treatment $p < 0.001$). On a dry weight basis, mild and severe Cd stress resulted in very similar values across the growth zone (Supplementary Fig. S4). However, in both cases Cd levels were highest at the base of the leaf, followed by a steep decline towards the mature tissues (segment $p < 0.001$; Fig. 2A). These findings indicate that dividing cells at the base of the leaf are exposed to higher amounts of Cd compared to later developmental stages.

Kinematic analysis

Cadmium accumulation in the leaf meristem suggested that, if the effect of Cd on leaf growth is caused by local accumulation in the growing tissues, cell division would be primarily responsible for the growth inhibition by Cd. To address this possibility, we performed a kinematic analysis to quantify the effects on cell division and cell elongation. We first determined the cell length profile for the epidermal cells directly adjacent to the stomatal files. In the first centimetre from the base of the leaf, cells were small and cell size decreased slightly, while their size steeply increased in the 2-4 centimetre region under severe Cd stress and in the 2-6 centimetre region under control conditions. Mature cell length was not affected by the treatments (Fig. 3A; Table 2).

The cell length data allowed us to calculate the velocity profile, which shows that the velocity at which cells move away from the base of the leaf gradually increases until it reaches a value equal to the leaf elongation rate at the end of the growth zone (Fig. 3B, Table 2). The derivative of the velocity curve yields relative cell expansion rates, which shows that increasing Cd levels progressively reduce the maximal expansion rates and the extent of the growth zone (Fig. 3C).

Because mature cell size is not affected, the decrease in leaf elongation rate (by 24 and 46% for mild and severe stress respectively in this experiment; $p < 0.001$; Table 2) was almost entirely caused by a reduced cell production rate (-21% and -43% for mild and severe stress, respectively; $p < 0.001$; Table 2). Cell production in turn, is determined by the number of dividing cells in the meristem and their cell division rate. Cadmium stress significantly reduced the number of cells in the meristem (by 17% in mild and 29% in severe stress; $p < 0.001$; Table 2) and cell division rate (by 5 and 19%, in mildly and severely stressed plants; $p = 0.058$; Table 2), which relates to an increased cell cycle duration (from 24 hours in control conditions to 26 and 30 hours in mild and severe stress, respectively; $p = 0.0317$; Table 2). Although mature cell length was not affected, the relative cell elongation rate was inhibited by Cd (by -13 and -33% for mild and severe stress, respectively; $p < 0.001$; Table 2). This reduction in cell elongation rate, however, was compensated for by an increased time cells spend in the elongation zone (12% and 45% for mildly and severely stressed plants, respectively, $p < 0.001$; Table 2). The reduced number of dividing cells was reflected by a significant decrease in the size of the meristem ($p = 0.001$; Table 2). As a consequence, the size of the growth zone as a

whole decreased from 70 mm down to 64 and 59 mm for plants under mild and severe treatment, respectively ($p = 0.054$; Table 2).

In summary, Cd inhibits leaf growth primarily by reducing the meristem size and inhibiting cell division and expansion rates.

Cadmium flux and deposition

The decreasing Cd concentration with increasing distance from the leaf base (Fig. 2A) could be a consequence of dilution by cell growth, raising the possibility that all Cd is taken up by the dividing cells at the base of the leaf (Supplementary Fig. S5 illustrates Cd dilution by growth). To verify this possibility, we used kinematics to calculate Cd deposition rates along the leaf growth zone.

Based on Cd concentration and tissue velocity, we calculated Cd flux and deposition rates. Cadmium flux, the bulk flow rate of Cd away from the leaf base, progressively increased in the first 6 to 7 centimetres, after which it became approximately constant (Fig. 2B) in both Cd treatments. Assuming steady state, the derivative of the flux curve yields the local rates of Cd deposition, which was highest at the base of the leaf where cells are actively dividing (Fig. 2C). Towards the end of the growth zone, high velocity (Fig. 3B) in combination with only minor changes in Cd concentration, caused relatively large fluctuations in flux and even more in deposition rates. We consider this artifacts. Nevertheless, our data show that although Cd concentrations rapidly drop once cells leave the division zone, deposition continues in elongating cells and stops around the end of the elongation zone.

Flow cytometry

To analyse which phase of the cell cycle was affected by Cd, explaining the increased cell cycle duration (Table 2), and to assess if there was an effect on endoreduplication in expanding cells, we performed flow cytometry on one-centimetre sections along the leaf base. The fraction of 4C cells relative to cells with a 2C DNA content was highest in the second centimetre of the leaf (Fig. 4A), where cells exit the meristem (Table 2). After an initial drop, DNA contents increased towards the end of the elongation zone, suggesting a limited amount of endoreduplication (Fig. 4A).

Furthermore, this analysis suggests active proliferation in the first 3 centimetres of the leaf for all treatments. This result appears in contrast with our kinematic analysis that shows a meristem size of 1 to 1.5 centimetres for the severely stressed and control leaves, respectively. This difference may be due to flow cytometry being performed on a mix of all cell types, while kinematics is based on epidermal pavement cells. Nevertheless, the reduced meristem size is clearly reflected in the more rapid drop of the 4C/2C ratio in the Cd-treated leaves. Consistent with active proliferation at the base and limited endoreduplication in the elongation zone, cells in S-phase could be detected throughout the growth zone, with the highest levels in the second centimetre (Fig. 4B).

The 4C/2C ratio was reduced by severe Cd stress, whereas the mild treatment was very similar to the control treatment. Severe Cd stress reduced the fraction of S-phase cells throughout the growth zone, whereas at the leaf base mild stress was similar to the control treatment, but in the elongation zone resembled the severe stress.

In conclusion, the flow cytometry data support a reduced meristem size and a reduced 4C/2C ratio under Cd stress, suggesting an inhibition of the G1/S transition in both mitotic and endoreduplicating cells.

Quantitative real-time PCR

To better understand the molecular mechanism explaining the inhibition of cell division by Cd, we analysed the expression levels of 3 cell cycle regulatory genes: *wee1*, *mcm4* and *cyclin-B2-4.* The overall expression pattern of these genes reflected the distribution of cell division activity and the inhibition by Cd (Table 2), with the highest expression levels around 1 centimetre from the base (Fig. 5). Severe Cd stress reduced the expression of these cell cycle regulators throughout the growth zone and caused a more rapid drop between 1.5 and 3.5 centimetres from the base, reflecting the reduced cell division rate and shortening of the meristem (Table 2), respectively. The response to mild stress was similar to the severe stress in the basal centimetre, whereas in more distal positions it appeared similar to the control condition.

Discussion

In order to answer our first research question, whether Cd could directly affect dividing and elongating cells in the growing maize leaf, we determined the Cd levels along the gradient of cell division and expansion at the base of the leaf into the mature blade tissue. Cd concentrations were highest at the base of the leaf, rapidly declined with increasing distance from the base and stabilised at around the 5th centimetre (Fig. 2A). This closely relates to our kinematics data, showing that the growth inhibition exerted by Cd is primarily caused by a reduced cell production in the meristem, located in the base of the leaf. Noteworthy, these observations demonstrate that whole leaf sampling, typically used to evaluate leaf Cd concentrations (e.g. Khaliq *et al.*, 2019; Masood *et al.*, 2016; Nada *et al.*, 2007; Shi *et al.*, 2019; Ye *et al*., 2018; Zhou *et al.*, 2018), underestimates the concentration in dividing and elongating cells .

Using kinematics, we were able to calculate Cd fluxes and Cd deposition rates. One possibility to account for the high levels of Cd in the meristem and their rapid decline in the elongation zone (Fig. 2A) could be that Cd is specifically deposited at the base of the leaf and diluted by cell expansion in the elongation zone. Under these circumstances, Cd flux in the elongation zone should remain constant, because the dilution of Cd and the increase in cellular velocity due to water uptake are directly proportional (Supplementary Fig. S5). However, we observed a steady increase in Cd flux until at least the 4th centimetre (Fig. 2B), demonstrating that Cd deposition continues in the elongation zone. Cadmium deposition rates in the elongation zone are lower than those of water driving cell expansion, explaining the decreasing Cd concentrations from the leaf base towards the blade (Fig. 2A). Thus, while deposition rates are highest in the meristem of the growing maize leaf, Cd continues to be deposited while cells are expanding (Fig. 2C), suggesting that in elongating cells Cd is (passively) taken up with the influx of water required to drive cell growth. Interestingly, plants exposed to a mild Cd dose have a higher Cd flux compared to severely stressed plants (Fig. 2B), even though concentrations are higher in leaves exposed to the highest concentration (Fig. 2A). This is because both segment fresh weight and velocity are higher under mild stress compared to severe stress, resulting in more tissue passing per unit time. When the flux is expressed on a fresh weight basis, compensating for the amount of tissue passing by (Supplementary Fig. S6), severely stressed plants have a slightly higher Cd flux.

The past decade, Cd deposition in the meristem received attention in the shoot of eudicotyledonous and *Graminae* plants using a positron-emitting tracer imaging system together with positron-emitting Cd to trace the translocation and accumulation of Cd throughout the plant. This technique also showed that in rice Cd already accumulated at the base of the leaf after 1 hour of tracer exposure, whereafter the signal also increased in the rest of the sheet and in the blade (Fujimaki *et al.*, 2010; Kobayashi *et al.*, 2013). Radioactive Cd deposition was also studied in *Arabidopsis thaliana*, where Dauthieu *et. al.* (2009) showed that Cd was deposited throughout young leaves and that the zone of deposition retracted towards the base and petiole in older leaves. Young dicotyledonous leaves first consist entirely out of dividing cells, after which a cell cycle arrest front appears at the tip of the growing leaf which moves towards the petiole (Andriankaja *et al.*, 2012). Therefore, the pattern of Cd deposition in these leaves also broadly coincides with cell proliferation. In addition to leaves, predominant accumulation of Cd in the meristem also occurs in roots of rice (Zhao *et al.*, 2013; Zhan *et al.*, 2017). Taken together, these results indicate that, during growth, Cd is mainly deposited and accumulated in dividing and elongating tissue.

Dividing and elongating tissue, acting as a Cd sink, is supported by the study performed by Kobayashi *et al.* (2013) on rice seedlings. They showed that the xylem transpiration stream facilitates Cd transport from the roots towards the shoot. However, once Cd reaches the base of the stem, it is loaded into the phloem at the nodes and mainly directed towards the young growing leaves. In the new leaves, Cd preferentially accumulated in the sheath (i.e. where the growth zone resides), whereas calcium was spread throughout the growing leaf.

To address our second research question, the cellular basis of Cd inhibited leaf growth in maize, we analysed the contribution of cell division and elongation to the growth inhibition by Cd. Our results indicate that Cd inhibited leaf growth by inhibiting cell production by up to 43 percent, while mature cell length remained largely unaffected. This is consistent with the meta-analysis performed by Gázquez and Beemster (2017), who showed that variations in meristematic cell number, rather than mature cell size, primarily determine organ size in plants. For *Graminae* leaves, they also showed that mature cell length is strictly controlled and does not contribute significantly to changes in leaf elongation rates, which matches the unaffected mature cell length in our analysis.

The main cause of a lower cell production rate in our study was a reduction in number of meristematic cells, resulting in shortening of the meristem size by up to 26 %. This reduced meristem size is consistent with Cd-induced meristem size reductions in roots of wheat, pea and Arabidopsis (Fusconi *et al.*, 2007; Pena *et al.*, 2012; Yuan and Huang, 2016; Bruno *et al.*, 2017). Although we confirmed the reduction in meristem in 3 independent experiments (i.e. kinematics study, quantitative real-time PCR of cell cycle genes and a flow cytometry study), there was discrepancy in the apparent meristem sizes. Based on our kinematics results data, meristem sizes ranged from 1 to 1.5 centimetres for severe to control condition respectively (Table 2), whereas cell cycle gene expression patterns suggested it to be considerably longer (up to 2.5 centimetres under control conditions when interpreting *cyclin-B2-4* expression data (Fig. 5)). In the flow cytometry results, the 4C/2C minimum at the meristem-elongation transition is reached 1 centimetre later by the control treatment (Fig. 4A), suggesting that cells are still dividing in the 2-to-3 centimetre segment under control conditions. This discrepancy between datasets can be related to the cell type studied by the different methodologies. In the kinematic analysis, epidermal pavement cells are studied, whereas in gene expression and flow cytometry study, whole leaf segments containing all cell types were used. Tardieu et al. (2000) showed that mesophyll cells can divide twice as long as epidermal cells, which could explain why the techniques which incorporate all cell types (i.e. quantitative real-time PCR and flow cytometry) result in longer meristems compared to kinematic analysis, which is based only on epidermal pavement cells. Nevertheless, all data consistently showed that Cd reduces maize leaf meristem size.

Besides a significant reduction in meristem cell number, cell cycle duration also increased from 24 hours under control conditions to 30 hours under severe stress conditions. This means that cells divided at a lower rate because they were halted at some point(s) in the cell division cycle. Inhibited cell cycle progression under Cd stress has previously been reported mainly in roots and synchronised cell culture experiments. In roots of *Arabidopsis thaliana*, Cd inhibited the cell cycle mainly at the G2/M transition, resulting in a relative increase in 4C nucleic content at the cost of 2C nuclei (Cui *et al.*, 2017; Cao *et al.*, 2018). No significant effect of Cd on the proportion of cells in the S-phase was reported by Cao *et al.* (2018). However, detrimental effects of Cd on the S-phase were shown in synchronised plant cell cultures, where Cd administration during S-phase delayed the mitosis by 2 hours in tobacco cells

(Kuthanova *et al.*, 2008) and Cd administration at the start of the cell cycle decreased the DNA-synthesis rate in soybean cells (Sobkowiak and Deckert, 2004). Also, in root apices of peas (*Pisum sativum L.*), Cd affected meristematic cells in the G1/S and G2/M transition, resulting in respectively less cells in the S- and M-phase. Inhibition of S-phase entry was also shown in a study on Cd stress in leaves of lettuce (Monteiro *et al.*, 2012). Though insignificant, Monteiro *et al.* (2012) showed an increase in percentage of G0/G1 cells, followed by a decrease in cells in the S-phase and G2-phase when grown under mild to severe Cd conditions (respectively 10 and 50 µM Cd). Cd-inhibited G1/S transition is consistent with our flow cytometry data in the meristem of the growing maize leaf, where we show a lower proportion of cells in the S-phase, together with an accumulation of cells with a 2C nucleic content (Fig. 4).

In order to better understand why cells were progressing slower through the cell cycle, we selected 3 key cell cycle genes, i.e. *wee1* and *mcm4* which have a function during the S-phase and *cyclin-B2-4*, a B-type cyclin controlling G2/M transition. *wee1*, a kinase of which transcript abundance peaks during S-phase progression (Cools *et al.*, 2011), controls cell cycle arrest upon DNA damage and is also important for meristem maintenance during replication stress (Hu *et al.*, 2016). Since Cd is linked to DNA damage in multiple studies (as reviewed by Huybrechts *et al.*, 2019), we expected *wee1* transcript levels to increase under Cd stress. Surprisingly, under severe Cd stress, expression levels of *wee1* were consistently lower compared to the control treatment over the entire meristem (Fig. 5). However, these results do reflect those of Cao *et al.* (2018) and Cui *et al.* (2017), who also found *wee1* downregulation under Cd stress in roots of Arabidopsis after 5 days of Cd exposure. Only low amounts of Cd caused a significant upregulation of *wee1* transcription (Cui *et al.*, 2017; Cao *et al.*, 2018).

We also found similar expression profiles for *mcm4* (helicase activity) and *cyclin-B2-4* (controlling G2/M transition), i.e. lower expression under severe Cd stress over the entire meristem compared to the control condition. Downregulation of B-type cyclins was also shown in the experiments of Cao *et al.* (2018) and Cui *et al.* (2017) and also in soybean suspension-culture cells, Cd reduced in *cyclin-B1* transcription (Sobkowiak and Deckert, 2003). Next, in Cd exposed shoots of wheat (*Triticum urartu*), 2 and 5 day Cd exposure

reduced expression levels of multiple MCMs (Qiao *et al.*, 2019), whereas 48 hour exposure to the same Cd dose decreased *mcm2* transcript levels in roots of wheat seedlings (Pena *et al.*, 2012). Downregulation of cell cycle-related genes by Cd seems to be common, as this was also supported by findings of Zhao *et al.* (2013) who reported that 12 out of 17 cell cycle-related genes had severely reduced transcript levels in Cd exposed rice roots.

Taken together, exposure to of Cd appears to stops cells from entering the cell cycle (i.e. inhibited G1/S transition), which is supported by the lower proportion of cells in S-phase and with the 4C nuclei content found in our study. With less cells entering the cell cycle, transcript levels of cell cycle-related genes could be relatively less abundant. We therefore hypothesize that under severe Cd stress, cells are hindered in entering the cell cycle in general, which could lead to an overall downregulation of most cell cycle genes.

Next, although mature cell length was unaffected, Cd significantly reduced relative cell elongation rate under severe stress. Nevertheless, cells did achieve the same mature cell length due to an increased time spent in the elongation zone. The inhibited cell elongation rate could be related to lower endopolyploidy levels in the elongation zone under severe stress, since DNA content is often linked to cell growth (Melaragno *et al.*, 1993; Sugimoto-Shirasu and Roberts, 2003) (Fig. 4). Based on our kinematics (Table 2) and cell cycle gene expression analysis (Fig. 5), we do not expect any cell division to occur further than 3 centimetres from the base of the leaf. Yet we do see a steady increase in 4C nuclei after this position, indicating a limited amount of endoreduplication to be present in the elongation zone. The endoreduplication process was negatively affected by our severe stress condition, where the 4C/2C ratio under severe stress stayed well below the one under control conditions over the entire elongation zone. However, the difference between control and severe Cd treatments on the 4C/2C ratio is quite constant from 1 to 7 centimetres, which could indicate that the process of endoreduplication itself is not really hampered, but the difference is there because a lower proportion of 4C nuclei was already present in the meristematic region under severe Cd stress. This difference in 4C/2C ratio is then retained throughout the elongation zone while the process of endoreduplication takes place at similar rates as in controls.

Because of the potential link between polyploidy level and cell growth, a reduced DNA content could negatively impact the process of cell elongation in the Cd exposed maize leaf

505 growth zone. Similar to our results, Hendrix *et al.* (2018) related a decreased cell surface area
506 to a lower extent of endoreduplication in leaves of Cd exposed Arabidopsis. However, in roots
507 of *Pisum sativum* and *Arabidopsis thaliana*, Cd exposure resulted in increased polyploidy
508 levels (Fusconi *et al.*, 2006; Repetto *et al.*, 2007; Cui *et al.*, 2017; Cao *et al.*, 2018). Therefore,
509 in a recent review by Huybrechts *et al.* (2019), it was suggested that Cd exposure stimulates
510 the endocycle in roots and inhibits it in leaves.

511

512 Lastly, it is remarkable that an eight-fold difference in Cd dose between mild and severe
513 treatments resulted in a limited difference in Cd accumulation throughout the growth zone
514 while the effects on growth, cellular and molecular processes were quite apparent. The
515 relatively small differences in accumulation could potentially be explained by a saturated
516 uptake and/or transport, to which the mild stress conditions might already get close. Related
517 to this saturated uptake, Huang *et al.* (2019) have shown that Cd uptake in rice increased
518 steeply under incremental low Cd concentrations, yet, at higher concentrations, Cd uptake
519 was levelling off when Cd concentrations further increased. It is not clear how a relatively
520 small difference in Cd accumulation (a maximal difference of 40% in the meristem between
521 mild and severe stress, t-test p-value: 0.11) could result in drastic differences in growth
522 response. Perhaps, a very tight threshold level is exceeded under severe stress conditions,
523 where the plant is still able to cope with the mild treatment and succumbs under severe
524 stress. Passing the threshold level might result in a different subcellular distribution, affecting
525 more and potentially important processes. Also, the impact of Cd on roots was not studied in
526 the research presented here. It is very well possible that, in addition to the effects of locally
527 accumulating Cd in the leaf, signals originating from the roots inhibit leaf growth. Therefore,
528 further research should be undertaken to explore whether potential long-distance signals and
529 potential threshold levels of metabolic and regulatory processes become affected. Comparing
530 the mild and severe Cd treatments may provide an interesting entry into this issue.

531

532 Conclusion

533 Our primary objective was to understand how Cd uptake by the roots inhibits leaf growth in
534 maize. We found that Cd inhibits leaf growth through a reduction of the meristematic cell

number and by impairing the cell cycle at the G1/S transition resulting in an increased cell cycle duration. In addition, Cd inhibited cell elongation, which might be related to lower ploidy levels under severe Cd stress. We also showed that Cd predominantly accumulates in the meristem and that deposition of Cd continues at lower rates throughout the elongation zone, which implies direct impact of Cd on the cell cycle and cell expansion in the maize leaf growth zone.

This study opens perspectives to further investigate the impact of Cd on the physiology of the leaf growth zone of a monocotyledonous leaf. We have shown in this study and earlier (Avramova *et al.*, 2015*b*) that the maize leaf model allows sampling at subzonal resolution for a wide range of analyses. This will allow us to determine how and to what extent changes in micro- and macronutrient levels, phytohormone profiles, energy metabolism, cell wall metabolism, etc. in the leaf growth zone further explain the regulatory mechanisms by which Cd inhibits leaf growth.

Supplementary

Data Availability Statement

The data supporting the findings of this study are available from the corresponding author, Gerrit T.S. Beemster, upon request.

Acknowledgements

This work was supported by the Research Foundation Flanders (FWO) by project funding for J.B. and M.H. [G0B6716N]. All authors participated in the conception of the topic. J.B. wrote the manuscript. G.B. edited the manuscript. J.B. made the figures and tables. J.B and L.B. performed the HR-ICP-MS measurements. M.H., S.H. and A.C. facilitated and helped with the flow cytometry measurements. We thank Geoffrey Hibbs and Leen Vandenberghe for their assistance with quantitative real-time PCR. All authors read and approved the final manuscript after critically revising it for important intellectual content. The authors declare that they have no conflicts of interest.

References

Andriankaja M, Dhondt S, DeBodt S, *et al.* 2012. Exit from Proliferation during Leaf Development in *Arabidopsis thaliana*: A Not-So-Gradual Process. Developmental Cell **22**, 64–78.

Avramova V, AbdElgawad H, Vasileva I, Petrova AS, Holek A, Mariën J, Asard H, Beemster GTS. 2017. High Antioxidant Activity Facilitates Maintenance of Cell Division in Leaves of Drought Tolerant Maize Hybrids. Frontiers in Plant Science **8**, 84.

Avramova V, AbdElgawad H, Zhang Z, *et al.* 2015*a*. Drought induces distinct growth response, protection, and recovery mechanisms in the maize leaf growth zone. Plant Physiology **169**, 1382–1396.

Avramova V, Sprangers K, Beemster GTS. 2015*b*. The Maize Leaf: Another Perspective on Growth Regulation. Trends in Plant Science **20**, 787–797.

Bi Y, Chen W, Zhang W, Zhou Q, Yun L, Xing D. 2009. Production of reactive oxygen species, impairment of photosynthetic function and dynamic changes in mitochondria are early events in cadmium-induced cell death in *Arabidopsis thaliana*. Biology of the Cell **101**, 629–643.

Bruno L, Pacenza M, Forgione I, Lamerton LR, Greco M, Chiappetta A, Bitonti MB. 2017. In Arabidopsis thaliana Cadmium Impact on the Growth of Primary Root by Altering SCR Expression and Auxin-Cytokinin Cross-Talk. Frontiers in Plant Science **8**, 1–13.

Cao X, Wang H, Zhuang D, *et al.* 2018. Roles of MSH2 and MSH6 in cadmium-induced G2/M checkpoint arrest in Arabidopsis roots. Chemosphere **201**, 586–594.

Cools T, Iantcheva A, Weimer AK, Boens S, Takahashi N, Maes S, Van den Daele H, Van Isterdael G, Schnittger A, De Veylder L. 2011. The *Arabidopsis thaliana* checkpoint kinase WEE1 protects against premature vascular differentiation during replication stress. The Plant Cell **23**, 1435–1448.

Crowell EF, Timpano H, Desprez T, Franssen-Verheijen T, Emons A-M, Höfte H, Vernhettes S. 2011. Differential regulation of cellulose orientation at the inner and outer face of epidermal cells in the Arabidopsis hypocotyl. The Plant Cell **23**, 2592–2605.

Cui W, Wang H, Song J, *et al.* 2017. Cell cycle arrest mediated by Cd-induced DNA damage in Arabidopsis root tips. Ecotoxicology and Environmental Safety **145**, 569–574.

Cuypers A, Keunen E, Bohler S, *et al.* 2012. Cadmium and copper stress induce a cellular oxidative challenge leading to damage versus signalling. Metal Toxicity in Plants: Perception, Signaling and Remediation. Berlin, Heidelberg: Springer Berlin Heidelberg, 65–90.

Cuypers A, Plusquin M, Remans T, *et al.* 2010. Cadmium stress: An oxidative challenge. BioMetals **23**, 927–940.

Dauthieu M, Denaix L, Nguyen C, Panfili F, Perrot F, Potin-Gautier M. 2009. Cadmium uptake and distribution in *Arabidopsis thaliana* exposed to low chronic concentrations depends on plant growth. Plant and Soil **322**, 239–249.

Fujimaki S, Suzui N, Ishioka NS, Kawachi N, Ito S, Chino M, Nakamura S. 2010. Tracing cadmium from culture to spikelet: noninvasive imaging and quantitative characterization of absorption, transport, and accumulation of cadmium in an intact rice plant. Plant Physiology **152**, 1796–1806.

Fusconi A, Gallo C, Camusso W. 2007. Effects of cadmium on root apical meristems of *Pisum sativum* L.: Cell viability, cell proliferation and microtubule pattern as suitable markers for assessment of stress pollution. Mutation Research - Genetic Toxicology and Environmental Mutagenesis **632**, 9–19.

Fusconi A, Repetto O, Bona E, Massa N, Gallo C, Dumas-Gaudot E, Berta G. 2006. Effects of cadmium on meristem activity and nucleus ploidy in roots of *Pisum sativum* L. cv. Frisson seedlings. Environmental and Experimental Botany **58**, 253–260.
Gázquez A, Beemster GTS. 2017. What determines organ size differences between species? A meta-analysis of the cellular basis. New Phytologist **215**, 299–308.
Green PB. 1962. Mechanism for Plant Cellular Morphogenesis. Science **138**, 1404–1405.
Hahne F, LeMeur N, Brinkman RR, Ellis B, Haaland P, Sarkar D, Spidlen J, Strain E, Gentleman R. 2009. flowCore: a Bioconductor package for high throughput flow cytometry. BMC Bioinformatics **10**, 106.
Hendrix S, Keunen E, Mertens AIG, Beemster GTS, Vangronsveld J, Cuypers A. 2018. Cell cycle regulation in different leaves of *Arabidopsis thaliana* plants grown under control and cadmium-exposed conditions. Environmental and Experimental Botany **155**, 441–452.
Hu Z, Cools T, De Veylder L. 2016. Mechanisms used by plants to cope with DNA damage. Annual Review of Plant Biology **67**, 439–462.
Huang L, Li WC, Tam NFY, Ye Z. 2019. Effects of root morphology and anatomy on cadmium uptake and translocation in rice (Oryza sativa L.). Journal of Environmental Sciences **75**, 296–306.
Huybrechts M, Cuypers A, Deckers J, Iven V, Vandionant S, Jozefczak M, Hendrix S. 2019. Cadmium and plant development: an agony from seed to seed. International Journal of Molecular Sciences **20**, 3971.
Kavanová M, Lattanzi FA, Grimoldi AA, Schnyder H. 2006. Phosphorus deficiency decreases cell division and elongation in grass leaves. Plant Physiology **141**, 766–775.
Khaliq MA, James B, Chen YH, Ahmed Saqib HS, Li HH, Jayasuriya P, Guo W. 2019. Uptake, translocation, and accumulation of Cd and its interaction with mineral nutrients (Fe, Zn, Ni, Ca, Mg) in upland rice. Chemosphere **215**, 916–924.
Kobayashi NI, Tanoi K, Hirose A, Nakanishi TM. 2013. Characterization of rapid intervascular transport of cadmium in rice stem by radioisotope imaging. Journal of Experimental Botany **64**, 507–517.
Kuthanova A, Fischer L, Nick P, Opatrny Z. 2008. Cell cycle phase-specific death response of tobacco BY-2 cell line to cadmium treatment. Plant, Cell & Environment **31**, 1634–1643.
Lin F, Jiang L, Liu Y, Lv Y, Dai H, Zhao H. 2014. Genome-wide identification of housekeeping genes in maize. Plant Molecular Biology **86**, 543–554.
Livak KJ, Schmittgen TD. 2001. Analysis of relative gene expression data using real-time quantitative PCR and the 2-ΔΔCT method. Methods **25**, 402–408.
Loix C, Huybrechts M, Vangronsveld J, Gielen M, Keunen E, Cuypers A. 2017. Reciprocal interactions between cadmium-induced cell wall responses and oxidative stress in plants. Frontiers in Plant Science **8**, 1–19.
Masai H, Matsumoto S, You Z, Yoshizawa-Sugata N, Oda M. 2010. Eukaryotic chromosome dna replication: where, when, and how? Annual Review of Biochemistry **79**, 89–130.
Masood A, Khan MIR, Fatma M, Asgher M, Per TS, Khan NA. 2016. Involvement of ethylene in gibberellic acid-induced sulfur assimilation, photosynthetic responses, and alleviation of cadmium stress in mustard. Plant Physiology and Biochemistry **104**, 1–10.
Meiri A, Silk WK, Läuchli A. 1992. Growth and deposition of inorganic nutrient elements in developing leaves of *Zea mays* L. Plant Physiology **99**, 972–978.
Melaragno JE, Mehrotra B, Coleman AW. 1993. Relationship between endopolyploidy and cell size in epidermal tissue of Arabidopsis. The Plant Cell **5**, 1661–1668.
Monteiro C, Santos C, Pinho S, Oliveira H, Pedrosa T, Dias MC. 2012. Cadmium-induced cyto-

and genotoxicity are organ-dependent in lettuce. Chemical Research in Toxicology **25**, 1423–1434.

Nada E, Ferjani BA, Ali R, Bechir BR, Imed M, Makki B. 2007. Cadmium-induced growth inhibition and alteration of biochemical parameters in almond seedlings grown in solution culture. Acta Physiologiae Plantarum **29**, 57–62.

Nagajyoti PC, Lee KD, Sreekanth TVM. 2010. Heavy metals, occurrence and toxicity for plants: a review. Environmental Chemistry Letters **8**, 199–216.

Nelissen H, Rymen B, Coppens F, Dhondt S, Fiorani F, Beemster GTS. 2013. Kinematic Analysis of Cell Division in Leaves of Mono- and Dicotyledonous Species: A Basis for Understanding Growth and Developing Refined Molecular Sampling Strategies. Plant Organogenesis: Methods and Protocols.247–264.

Pena LB, Barcia RA, Azpilicueta CE, Méndez AAE, Gallego SM. 2012. Oxidative post translational modifications of proteins related to cell cycle are involved in cadmium toxicity in wheat seedlings. Plant Science **196**, 1–7.

Qiao K, Liang S, Wang F, Wang H, Hu Z, Chai T. 2019. Effects of cadmium toxicity on diploid wheat (*Triticum urartu*) and the molecular mechanism of the cadmium response. Journal of Hazardous Materials **374**, 1–10.

Repetto O, Massa N, Gianinazzi-Pearson V, Dumas-Gaudot E, Berta G. 2007. Cadmium effects on populations of root nuclei in two pea genotypes inoculated or not with the arbuscular mycorrhizal fungus Glomus mosseae. Mycorrhiza **17**, 111–120.

Rymen B, Coppens F, Dhondt S, Fiorani F, Beemster GTS. 2010. Kinematic Analysis of Cell Division and Expansion. Plant Developmental Biology.203–227.

Scholes DR, Paige KN. 2015. Plasticity in ploidy: a generalized response to stress. Trends in Plant Science **20**, 165–175.

Scofield S, Jones A, Murray JAH. 2014. The plant cell cycle in context. Journal of Experimental Botany **65**, 2557–2562.

Shi GL, Li DJ, Wang YF, Liu CH, Hu ZB, Lou LQ, Rengel Z, Cai QS. 2019. Accumulation and distribution of arsenic and cadmium in winter wheat (*Triticum aestivum* L.) at different developmental stages. Science of The Total Environment **667**, 532–539.

Silva SAE, Techio VH, De Castro EM, De Faria MR, Palmieri MJ. 2013. Reproductive, cellular, and anatomical alterations in *pistia stratiotes* L. plants exposed to cadmium. Water, Air, and Soil Pollution **224**.

Sobkowiak R, Deckert J. 2003. Cadmium-induced changes in growth and cell cycle gene expression in suspension-culture cells of soybean. Plant Physiology and Biochemistry **41**, 767–772.

Sobkowiak R, Deckert J. 2004. The effect of cadmium on cell cycle control in suspension culture cells of soybean. Acta Physiologiae Plantarum **26**, 335–344.

Sprangers K, Avramova V, Beemster GTS. 2016. Kinematic Analysis of Cell Division and Expansion: Quantifying the Cellular Basis of Growth and Sampling Developmental Zones in *Zea mays* Leaves. Journal of Visualized Experiments, 1–11.

Sugimoto-Shirasu K, Roberts K. 2003. “Big it up”: endoreduplication and cell-size control in plants. Current Opinion in Plant Biology **6**, 544–553.

Tardieu F, Reymond M, Hamard P, Granier C, Muller B. 2000. Spatial distributions of expansion rate, cell division rate and cell size in maize leaves: a synthesis of the effects of soil water status, evaporative demand and temperature. Journal of Experimental Botany **51**, 1505–1514.

Verbruggen N, Hermans C, Schat H. 2009. Mechanisms to cope with arsenic or cadmium

excess in plants. Current Opinion in Plant Biology **12**, 364–372.
West G, Inzé D, Beemster GTS. 2004. Cell cycle modulation in the response of the primary root of arabidopsis to salt stress. Plant Physiology **135**, 1050–1058.
Ye W, Guo G, Wu F, Fan T, Lu H, Chen H, Li X, Ma Y. 2018. Absorption, translocation, and detoxification of Cd in two different castor bean (*Ricinus communis* L.) cultivars. Environmental Science and Pollution Research **25**, 28899–28906.
Yuan H-M, Huang X. 2016. Inhibition of root meristem growth by cadmium involves nitric oxide-mediated repression of auxin accumulation and signalling in Arabidopsis. Plant, Cell & Environment **39**, 120–135.
Zhan Y, Zhang C, Zheng Q, Huang Z, Yu C. 2017. Cadmium stress inhibits the growth of primary roots by interfering auxin homeostasis in *Sorghum bicolor* seedlings. Journal of Plant Biology **60**, 593–603.
Zhao FY, Hu F, Zhang SY, Wang K, Zhang CR, Liu T. 2013. MAPKs regulate root growth by influencing auxin signaling and cell cycle-related gene expression in cadmium-stressed rice. Environmental Science and Pollution Research **20**, 5449–5460.
Zhou H, Zhu W, Yang W-T, Gu J-F, Gao Z-X, Chen L-W, Du W-Q, Zhang P, Peng P-Q, Liao B-H. 2018. Cadmium uptake, accumulation, and remobilization in iron plaque and rice tissues at different growth stages. Ecotoxicology and Environmental Safety **152**, 91–97.

Tables

Table 1. Cd concentrations used in the experiments. Six different Cd doses were used for dose-response experiments, of which 3 treatments were selected for the detailed analyses in subsequent experiments.

Selected treatments (subsequent experiments)	**Cadmium concentration in the 10 ml spiking solutions (mmol/l)**	**Cadmium concentration in wet soil (mg Cd / kg wet soil)**	**Cadmium concentration in dry soil (mg Cd / kg dry soil)**
Control	0	0	0
Mild	11.6	20	46.5
	23.1	40	93.0
	46.3	80	186.0
Severe	92.5	160	372.1
	115.7	200	465.1
	138.8	240	558.1

Table 2. Kinematic analysis of the effect of Cd on cell division and cell expansion in the growing maize leaf. Mild and severe treatment are compared to the control treatment and the difference is expressed as a percentage of the control values. Data are based on cells in a representative file of epidermal pavement cells directly adjacent to a stomatal file. * indicates significantly different ($p < 0.05$). Data are mean values ± SE (n = 10-11 for LER, n = 4-5 for FLL, n = 6 for the other parameters).

Parameter	Control	Mild	Severe	Percentage change in Mild/Severe stress
Final leaf length (mm)	761 ± 16	634 ± 26	576 ± 47	-17* / -24*
Leaf elongation rate ($mm \cdot h^{-1}$)	3.23 ± 0.03	2.47 ± 0.05	1.74 ± 0.07	-24* / -46*
Length of the meristem (mm)	14.3 ± 0.7	12.2 ± 0.5	10.6 ± 0.5	-15* / -26*
Length of the elongation zone (mm)	56 ± 3	51 ± 3	48 ± 4	-8 / -14
Length of the growth zone (mm)	70 ± 3	64 ± 3	59 ± 4	-10 / -16
Length cells leaving meristem (µm)	18.0 ± 0.4	18.7 ± 0.4	18.5 ± 0.6	+4 / +3
Mature cell length (µm)	129 ± 3	127 ± 2	123 ± 3	-2 / -4
Number of cells in meristem	873 ± 43	720 ± 36	618 ± 32	-17* / -29*
Number of cells in elongation zone	999 ± 22	881 ± 31	829 ± 47	-12 / -17*
Number of cells in total growth zone	1872 ± 52	1602 ± 24	1448 ± 46	-14* / -23*
Cell production rate ($cells \cdot h^{-1}$)	25.0 ± 0.7	19.6 ± 0.4	14.2 ± 0.2	-21* / -43*
Cell division rate ($cells \cdot cell^{-1} \cdot h^{-1}$)	0.029 ± 0.002	0.028 ± 0.001	0.023 ± 0.002	-5 / -19
Relative cell expansion rate ($\mu m \cdot \mu m^{-1} \cdot h^{-1}$)	0.049 ± 0.002	0.043 ± 0.002	0.033 ± 0.002	-13 / -33*
Cell cycle duration (h)	24 ± 1	26 ± 1	30 ± 2	+5 / +25*
Time cells spend in the meristem (h)	238 ± 15	242 ± 13	282 ± 20	+2 / +19
Time cells spend in the elongation zone (h)	40 ± 2	45 ± 2	58 ± 3	+12 / +45*

Figure legends

Figure 1. The effect of Cd dose on leaf elongation rate (LER, A) and final length (FLL, B) of the fifth leaf of maize seedlings. The percentages indicate the values for each treatment relative to the control treatment. The fifth leaf was measured daily after its emergence from the whorl of older leaves. LER for individual plants was determined over the first 4 days after leaf emergence. Data are mean values ± SE (n = 7).

Figure 2. Cadmium concentration, flux and deposition along the growth zone of the maize leaf. The maize leaf growth zone was subdivided in 10 one-centimetre segments, starting from the base of the leaf. Blade segments were included in the Cd concentration measurements. **A.** Cadmium concentration based on fresh weight. Statistics for severe versus mild treatment (on $\log_{10}$ transformed data): $p_{treatment} < 0.001$, $p_{segment} < 0.001$, $p_{interaction\ treatment:segment} = 0.499$. **B.** Cadmium flux. This parameter illustrates the amount of Cd passing a position in the growth zone per day. Statistics for severe versus mild treatment: $p_{treatment} < 0.001$, $p_{segment} < 0.001$, $p_{interaction\ treatment:segment} < 0.001$. **C.** Cadmium deposition rates. This parameter is the local derivative (i.e. slope) of Cd flux. Towards the end of the growth zone, high velocity (plot B) in combination with only minor changes in Cd concentration (plot A), causes relatively large fluctuations in flux and even more in deposition rates. We consider this artifacts. Statistics for severe versus mild treatment: $p_{treatment} < 0.001$, $p_{segment} < 0.001$, $p_{interaction\ treatment:segment} < 0.001$. Data shown are mean values ± SE (n = 5 (A), 24-30 (B), 24-30 (C)). SEs smaller than the symbol size are not plotted.

Figure 3. Kinematic analysis of the effect of Cd on cell growth in the maize leaf growth zone. **A.** Average cell size at each mm of the growth zone. For related statistics, we refer to the kinematic analysis (Table 2) where the impact of Cd treatment on cell length (cells leaving the meristem and mature cell length) is presented. **B.** Tissue velocity at each mm of the growth zone. For related statistics, we refer to the kinematic analysis (Table 2) where the impact of Cd treatment on velocity, i.e. leaf elongation rate, is presented. Leaf elongation rate corresponds to the maximum velocity reached in this graph. **C.** The relative cell expansion rates (rel. cell exp. rate). For related statistics, we refer to the kinematic analysis (Table 2) where the average relative cell expansion rates are presented. Data shown are mean values ± SE (n = 6). SEs smaller than the symbol size are not plotted.

Figure 4. Flow cytometry analysis of the effect of Cd in the growth zone of maize leaves. The growth zone was subdivided in 10 one-centimetre segments, starting from the base of the leaf. **A.** Ratio 4C nuclei to 2C nuclei throughout the maize leaf growth zone. Statistics (data $\log_{10}$-transformed, two-way ANOVA): $p_{treatment} < 0.001$, $p_{segment} < 0.001$, $p_{interaction\ treatment:segment} = 0.611$. **B.** Percentage of nuclei in the S-phase throughout the maize leaf growth zone. Statistics (two-way ANOVA): $p_{treatment} < 0.001$, $p_{segment} < 0.001$, $p_{interaction\ treatment:segment} = 0.004$. Data shown are mean values ± SE (n = 6). SEs smaller than the symbol size are not plotted.

Figure 5. The effect of Cd on cell cycle gene expression in the growth zone of maize leaves. The first 3 centimetres were subdivided in half centimetre segments, while the remaining two centimetres were segmented in one centimetre pieces. Fold gene expression is calculated relatively to the expression level of the control treatment's first segment. Statistics: data $\log_{10}$ transformed, two-way ANOVA $p_{treatment} < 0.001$, $p_{segment} < 0.001$ and $p_{interaction\ treatment:segment} < 0.001$. Data shown are mean values ± SE (n = 3). SEs smaller than the symbol size are not plotted.

Figures

Figure 1.

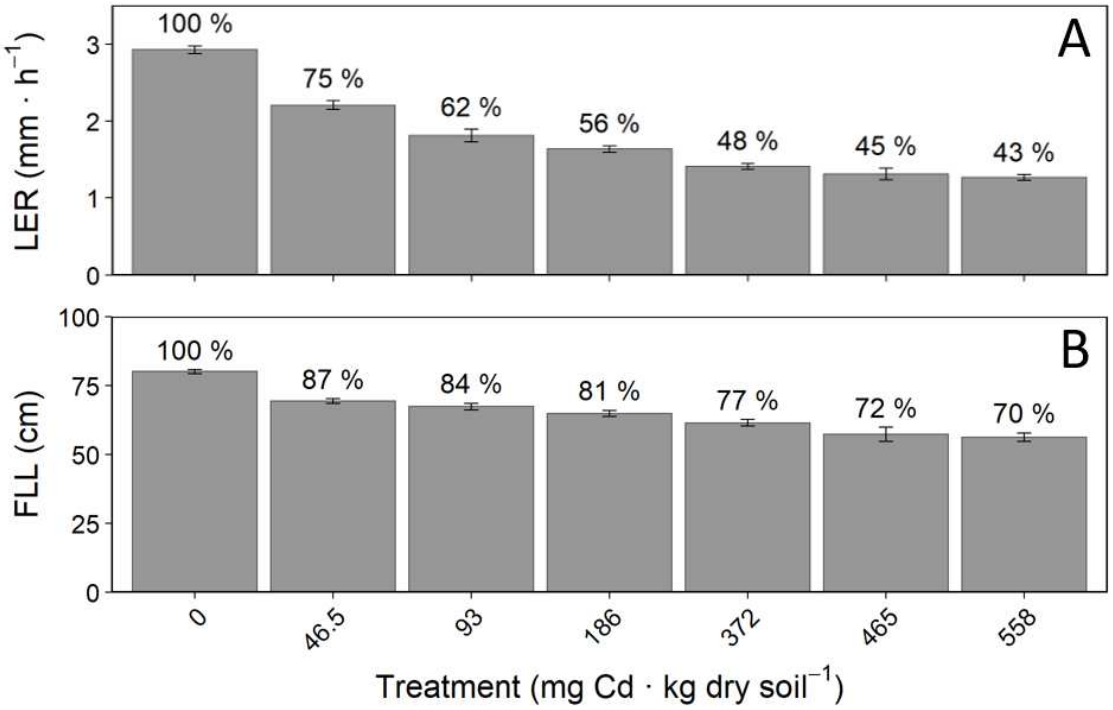

Figure 2

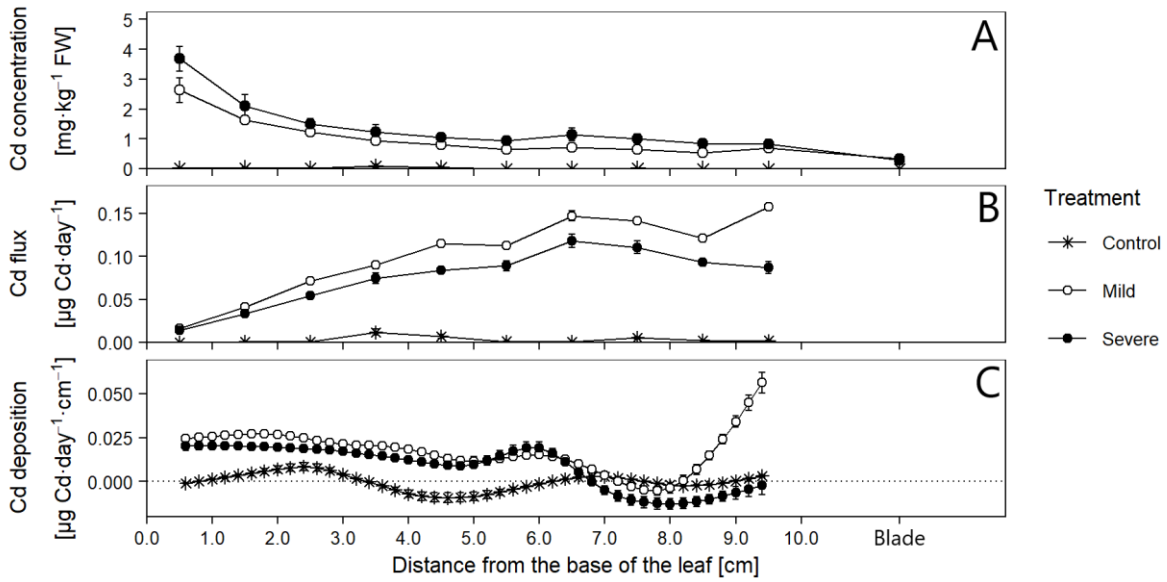
Cd concentration
[mg·kg⁻¹ FW]
A
Cd flux
[µg Cd·day⁻¹]
B
Cd deposition
[µg Cd·day⁻¹·cm⁻¹]
C
Distance from the base of the leaf [cm]
Blade
Treatment
Control
Mild
Severe

Figure 3

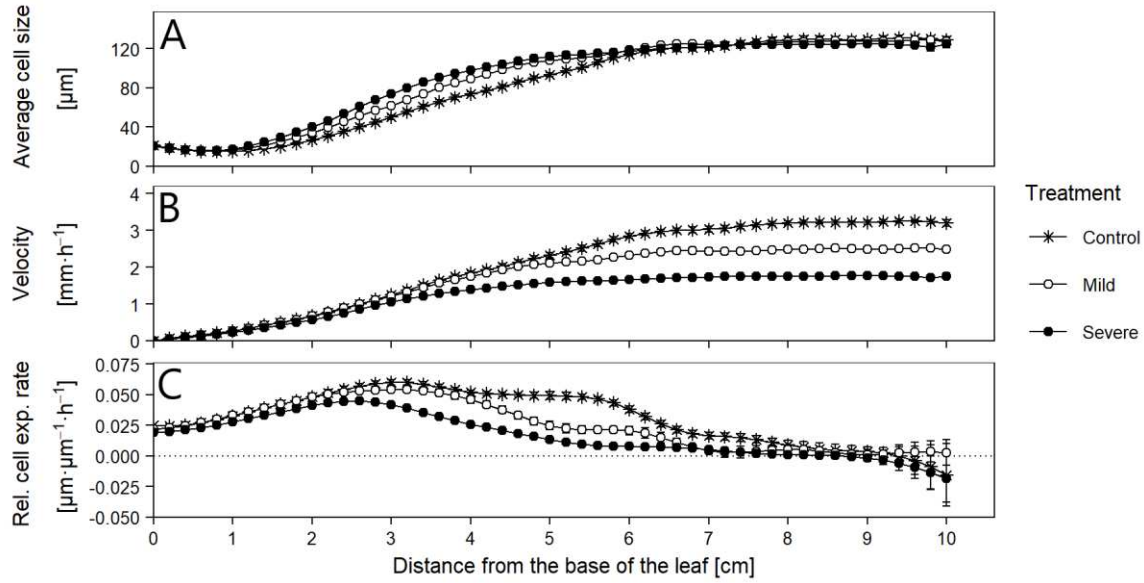
A
B
C
Average cell size [µm]
Velocity [mm·h⁻¹]
Rel. cell exp. rate [µm·µm⁻¹·h⁻¹]
Distance from the base of the leaf [cm]
Treatment
Control
Mild
Severe

Figure 4

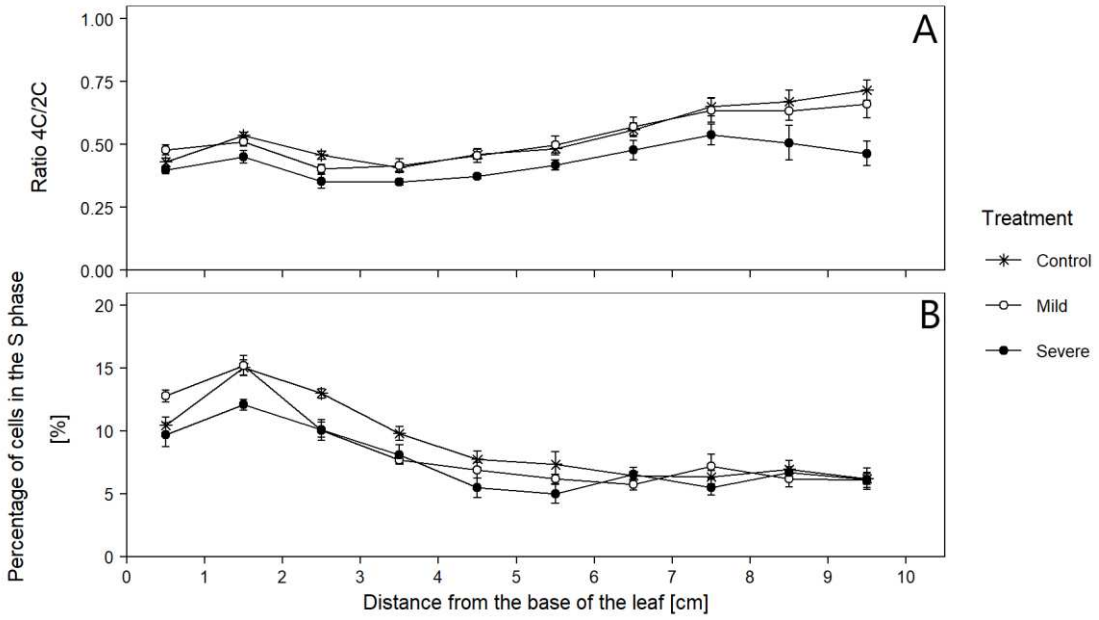
A
B
Ratio 4C/2C
Percentage of cells in the S phase [%]
Distance from the base of the leaf [cm]
Treatment
Control
Mild
Severe

Figure 5

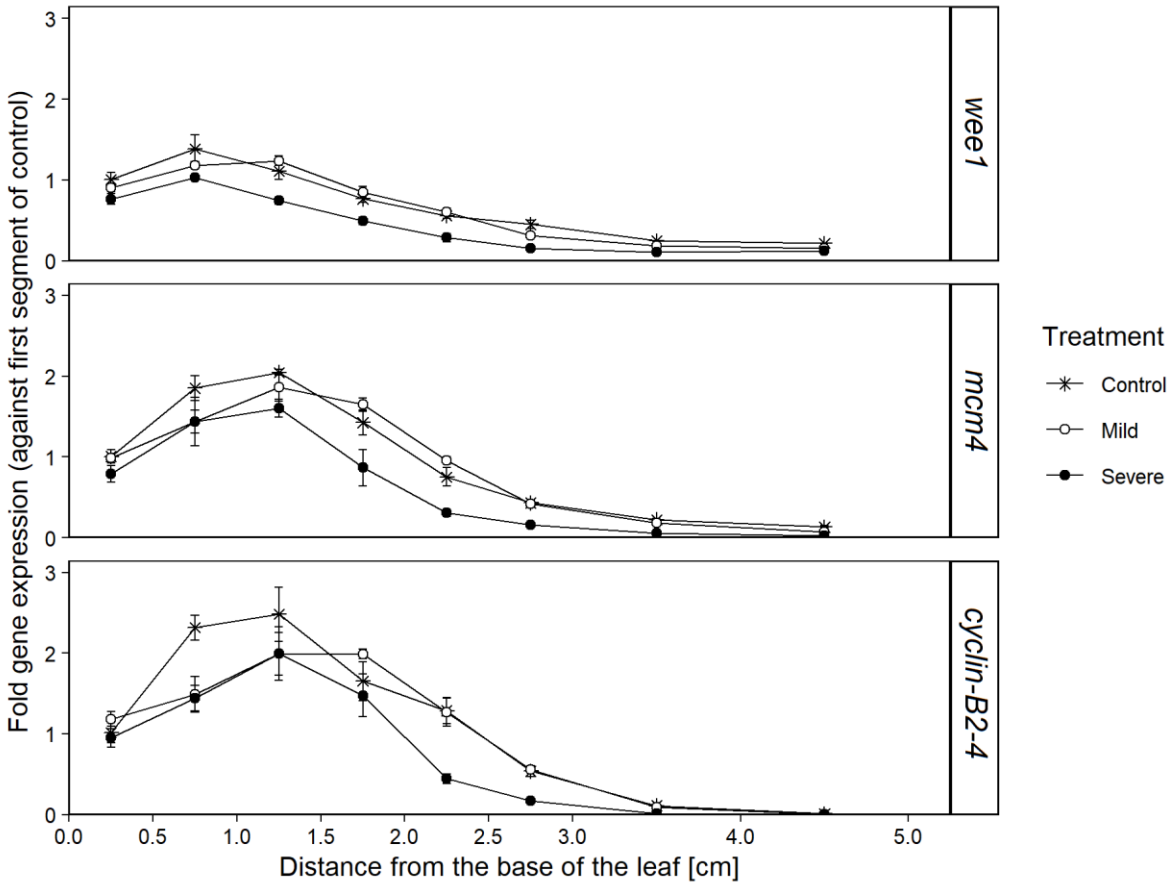
wee1
mcm4
cyclin-B2-4
Fold gene expression (against first segment of control)
Distance from the base of the leaf [cm]
Treatment
Control
Mild
Severe